Published in final edited form as:

Angew Chem Int Ed Engl. 2016 June 20; 55(26): 7520–7524. doi:10.1002/anie.201601902.

Design of Switchable Chimeric Antigen Receptor T Cells Targeting Breast Cancer

Yu Cao Dr.,
Department of Chemistry and The Skaggs Institute for Chemical Biology, The Scripps Research Institute, 10550 N Torrey Pines Rd, La Jolla, CA, 92037 (USA)

David T. Rodgers Dr.,
California Institute for Biomedical Research, 11119 N Torrey Pines Rd, La Jolla, CA, 92037 (USA)

Juanjuan Du Dr.,
California Institute for Biomedical Research, 11119 N Torrey Pines Rd, La Jolla, CA, 92037 (USA)

Insha Ahmad Dr.,
Department of Chemistry and The Skaggs Institute for Chemical Biology, The Scripps Research Institute, 10550 N Torrey Pines Rd, La Jolla, CA, 92037 (USA)

Eric N. Hampton Dr.,
California Institute for Biomedical Research, 11119 N Torrey Pines Rd, La Jolla, CA, 92037 (USA)

Jennifer S. Y. Ma Dr.,
California Institute for Biomedical Research, 11119 N Torrey Pines Rd, La Jolla, CA, 92037 (USA)

Magdalena Mazagova Dr.,
California Institute for Biomedical Research, 11119 N Torrey Pines Rd, La Jolla, CA, 92037 (USA)

Sei-hyun Choi Dr.[+],
Department of Chemistry and The Skaggs Institute for Chemical Biology, The Scripps Research Institute, 10550 N Torrey Pines Rd, La Jolla, CA, 92037 (USA)

Hwa Young Yun Dr.,
Department of Chemistry and The Skaggs Institute for Chemical Biology, The Scripps Research Institute, 10550 N Torrey Pines Rd, La Jolla, CA, 92037 (USA)

Han Xiao Dr.,
Department of Chemistry and The Skaggs Institute for Chemical Biology, The Scripps Research Institute, 10550 N Torrey Pines Rd, La Jolla, CA, 92037 (USA)

Pengyu Yang Dr.,
California Institute for Biomedical Research, 11119 N Torrey Pines Rd, La Jolla, CA, 92037 (USA)

Xiaozhou Luo Dr.,
Department of Chemistry and The Skaggs Institute for Chemical Biology, The Scripps Research Institute, 10550 N Torrey Pines Rd, La Jolla, CA, 92037 (USA)

Correspondence to: Chan Hyuk Kim, Dr.; Peter G. Schultz, Prof.; Travis S. Young, Dr..

[+]Present address: Daegu-Gyeongbook Medical Innovation Center, 80 Chembok-ro, Dong-gu, Daegu, Korea, 41061.

Supporting information for this article is available on the WWW under http://www.angewandte.org

Reyna K. V. Lim Dr.,
California Institute for Biomedical Research, 11119 N Torrey Pines Rd, La Jolla, CA, 92037 (USA)

Holly M. Pugh Dr.,
California Institute for Biomedical Research, 11119 N Torrey Pines Rd, La Jolla, CA, 92037 (USA)

Feng Wang Dr.,
California Institute for Biomedical Research, 11119 N Torrey Pines Rd, La Jolla, CA, 92037 (USA)

Stephanie A. Kazane Dr.,
California Institute for Biomedical Research, 11119 N Torrey Pines Rd, La Jolla, CA, 92037 (USA)

Timothy M. Wright Dr.,
California Institute for Biomedical Research, 11119 N Torrey Pines Rd, La Jolla, CA, 92037 (USA)

Chan Hyuk Kim Dr.,
California Institute for Biomedical Research, 11119 N Torrey Pines Rd, La Jolla, CA, 92037 (USA)

Peter G. Schultz Prof., and
Department of Chemistry and The Skaggs Institute for Chemical Biology, The Scripps Research Institute, 10550 N Torrey Pines Rd, La Jolla, CA, 92037 (USA)

California Institute for Biomedical Research, 11119 N Torrey Pines Rd, La Jolla, CA, 92037 (USA)

Travis S. Young Dr.
California Institute for Biomedical Research, 11119 N Torrey Pines Rd, La Jolla, CA, 92037 (USA)

Abstract

Chimeric antigen receptor T (CAR-T) cells have demonstrated promising results against hematological malignancies but have encountered significant challenges in translation to solid tumors. To overcome these hurdles, we have developed a switchable CAR-T cell platform in which the activity of the engineered cell is controlled by dosage of an antibody-based switch. Here, we apply this approach to Her2 expressing breast cancers by engineering switch molecules through site-specific incorporation of FITC or grafting of a peptide neo-epitope (PNE) into the anti-Her2 antibody trastuzumab (clone 4D5). We demonstrate that both switch formats can be readily optimized to redirect CAR-T cells (specific for the corresponding FITC or peptide epitope) to Her2 expressing tumor cells and afford dose-titratable activation of CAR-T cells ex vivo and complete clearance of tumor in rodent xenograft models. This strategy may facilitate the application of immunotherapy to solid tumors by affording comparable efficacy with improved safety owing to switch-based control of the CAR-T response.

Graphical abstract

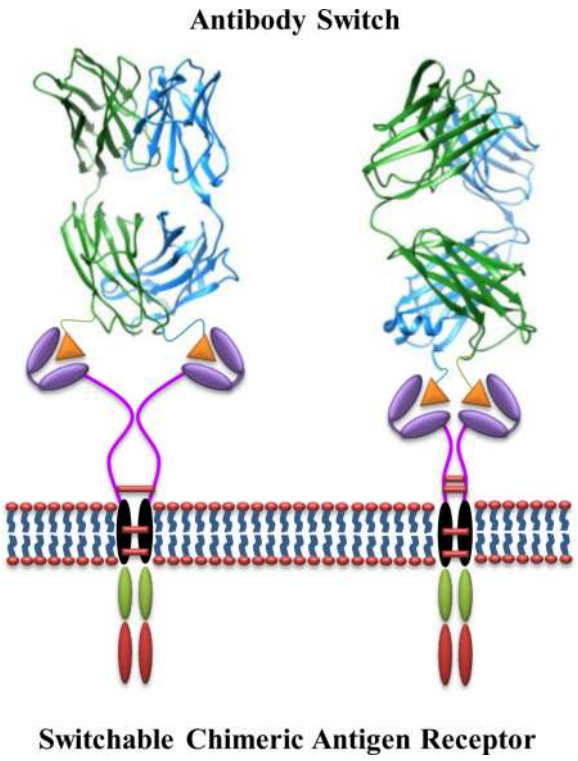

Keywords

chimeric antigen receptor; antibody switch; FITC; peptide neo-epitope; Her2 expressing breast cancer; unnatural amino acid

Adoptive immunotherapy using chimeric antigen receptor T cells is a promising new approach for cancer treatment[1–3]. Clinical trials have demonstrated marked antitumor responses for patients with hematological malignances, including those who have failed conventional therapies[4–7]. Despite these promising early results, significant challenges still exist. For example, leukemia and lymphoma patients treated with CD19 specific CAR-T cells have suffered severe cytokine release syndrome (CRS) due to the rapid activation and expansion of CAR-T cells on encountering CD19-positive cells, and can suffer long term B-cell aplasia due to the persistence of the CAR-T response[4;8;9]. The treatment of solid tumors has proven even more problematic due to on-target, off-tumor activity of CAR-T cells which has resulted in damage to healthy tissue[10]. In other solid tumor trials, CAR-T cells have demonstrated insufficient efficacy[11;12]. Thus, it has become increasingly appreciated that the treatment of solid tumors with CAR-T cell therapy requires robust methods for systematically optimizing and precisely controlling the engineered cells to provide an effective therapy with mitigated risks to the patient. One method that has been proposed is safety switches that can eliminate engineered cells in the case of an adverse event[13]. However, this strategy results in irreversible loss of therapeutic cells from circulation and does not solve the intrinsic lack of control associated with initiation of CAR-T cell therapy.

To control CAR-T cell activation, we and others have previously developed antibody-based switch molecules that control the activation, antigen specificity, and phenotype of CAR-T cells by the formation of a switch dependent immunological synapse[14–16]. This switchable CAR-T (sCAR-T) cell platform relies on a sCAR that is specific for a bio-orthogonal antigen (not present in normal tissue), and a recombinant antibody-based switch that confers tumor specificity and also contains the sCAR antigen. The activity of these sCAR-T cells is entirely dependent on the presence of the switch molecule. Recently, we reported the development of two sCAR platforms that utilize either semi-synthetic switches, generated by site-specific chemical conjugation of the targeting antibody with the small molecule fluorescein isothiocyanate (FITC), or fully recombinant switches constructed from genetic fusion of the targeting antibody with a short peptide neo-epitope (PNE) derived from the GCN4 peptide sequence)[15;16]. sCAR-T cells redirected by either FITC or PNE tagged switches efficiently cleared $CD19^+$ Nalm-6 tumors in murine xenograft models with reduced cytotoxicity by virtue of the ability to titrate the sCAR-T cell response; in addition, sCAR-T activity could be terminated by removal of the switch. Moreover, this platform can allow one universal CAR-T cell to be redirected to target heterogeneous or resistant tumors with multiple distinct switches, which should further improve the effectiveness of this therapeutic modality[15–19].

Herein, we extend this methodology to target Her2-expressing breast cancer cells. To generate anti-Her2 switches, the FITC or PNE peptide was introduced into the anti-Her2 antibody fragment Fab (clone 4D5) at defined sites in the variable or constant regions. These positions were chosen to vary the distance and orientation between the CAR and tumor antigen in order to optimize immunological synapse activity. For the FITC-based switches, a bio-orthogonal genetically encoded unnatural amino acid was used to site-specifically conjugate FITC to 4D5 Fab. Briefly, a mutant 4D5 Fab with a TAG nonsense codon at the desired sites was co-expressed in *Escherichia coli* (*E.coli*) with an orthogonal *Methanococcus jannaschii*-derived tRNA/aminoacyl-tRNA synthetase pair that selectively incorporates p-azidophenylalanine (pAzF) into proteins in response to the TAG codon. Based on previous experiments, pAzF was individually incorporated at light chain residues (LG68X or LS202X), or heavy chain residues (HS75X or HK136X) to generate four monovalent switches (Figure 1A)[15]. In addition, two bivalent switches were constructed with pAzF at both LG68X and HS75X, or LS202X and HK136X. To conjugate FITC to the Fab, a linker-modified FITC molecule containing a cyclooctyne group (BCN-PEG4-FITC) was attached via “Click” reaction[20;21] (Supplementary Fig. S1). Conjugation reactions proceeded to >95% completion as determined by SDS-PAGE gel (Supplementary Fig. S2A) and mass spectrometry (MS) (Supplementary Fig. S3 and Supplementary Table S1).

To generate PNE switch molecules, we grafted the PNE peptide sequence to the N- or C-terminus of the 4D5 Fab heavy chain or light chains to create the light chain N-terminal (LCNT), light chain C-terminal (LCCT), heavy chain N-terminal (HCNT) or heavy chain C-terminal (HCCT) switches (Figure 1A). A GGGGS peptide linker was used to separate the peptide tag from the Fab. To create bivalent switches, the PNE was grafted onto either the N- or C-terminus of the heavy and light chain to create NTBV or CTBV, respectively (Fig. 1A). Proteins were expressed in HEK293 suspension cells and further purified to > 95% homogeneity as confirmed by SDS-PAGE gel (Supplementary Fig. S2B). MS analysis

confirmed that the PNE fusions were not subject to post-translational modification or proteolysis (Supplementary Fig. S4 and Supplementary Table S2).

The binding affinity of all switches to SKBR3 (Her2 3+, clinical immunohistochemistry score), MDA MB453 (Her2 2+), MDA MB231 and MDA MB435 (Her2 1+) and MDA MB468 (Her2 0)[22], was assessed by flow cytometry. As shown in Supplementary Fig. S5, FITC and PNE-based switches bind to Her2 expressing cancer cells to a similar extent as wild type 4D5 Fab (Supplementary Table S3 and S4). Importantly, these switch molecules did not bind to Her2 0 MDA MB468 (lacking Her2 expression) cancer cells, confirming the specificity of the modified 4D5 Fab-based switches.

We have previously engineered sCARs using high affinity scFvs for FITC or the PNE[23;24] in 4-1BB-based second generation CAR backbones[25] (Figure 1B). For the PNE sCAR we further showed a short 12 amino acid hinge region (which connects the scFv to the transmembrane domain) derived from a dimeric mutant (S228P) of the IgG4 hinge (IgG4m) afforded greater activity than a longer 45 amino acid CD8 hinge region which is used in many conventional CAR constructs[16]. Therefore for both the FITC and PNE sCARs, we generated constructs harboring both the IgG4m and CD8 hinges (Figure 1B). Comparable sCAR expression (transduction efficiency of ~60%) for all four constructs on the surface of T cells was confirmed by flow cytometry, consistent with previous results[15;16]. We then tested the ability of the sCAR-T cells with CD8 or IgG4m hinges to bind their corresponding anti-Her2 switches. As shown in Supplementary Fig. S6 and S7, all the switches, bound to their corresponding sCAR-T cells with similar affinities. The wild type 4D5 Fab or an irrelevant switch antibody, did not bind to either sCAR-T cell, demonstrating the specificity of the sCARs for their respective tags (Supplementary Fig. S8).

To determine the optimal switch/sCAR combination for targeting Her2-expressing cells, we measured sCAR-T cells activation with monovalent (HS75X and LS202X for FITC; HCNT and LCCT for PNE) and bivalent (LG68X/HS75X and LS202X/HK136X for FITC; NTBV and CTBV for PNE) switches against breast cancer cells with varying levels of Her2 expression. In general, switches with FITC or PNE placed distal to the antigen domain provided the greatest activation. This result is consistent with the membrane proximal epitope of the Her2 specific Fab (vs the more membrane distal epitope of the CD19 specific Fab used in the previous studies) which likely requires extended distance between the sCAR-T cell and target cell to achieve optimal synapse geometry. The bivalent LS202X/HK136X conjugates induced the highest sCAR-T activation and this trend was most apparent on Her2 1+ cancer cells. As shown in Supplementary Fig. S9, the CD8 hinge-based anti-FITC CAR-T cells afforded greater sCAR-T cell activation than the IgG4m hinge-based sCAR-T cells for all the FITC switch designs, as determined by CD69/CD25 upregulation and inflammatory cytokine release (IL-2, IFN-γ and TNF-α). Interestingly, the same hinge was not optimal for all representative PNE-based switches tested (Supplementary Fig. S10). The anti-PNE sCAR harboring the CD8 hinge showed the greatest T cell activation and cytokine release when used with N-terminal (HCNT) PNE switches, but when the PNE was grafted onto the C-terminus (LCCT), the IgG4m hinge-based anti-PNE sCAR showed the best response. In agreement with the T-cell activation results, anti-FITC sCAR-T cells with the CD8 hinge were more cytotoxic than those with the IgG4m hinge (Fig. 2A), while anti-

PNE sCAR-T cells with the IgG4m hinge were more cytotoxic than those with the CD8 hinge (Fig. 2B). Notably, differences in cytotoxicity for CD8 vs IgG4m hinges were most apparent for Her2 1+ compared with Her2 3+ and Her2 2+ cells (Supplementary Fig. S11). The small number of immunological synapses formed by the low antigen density cells likely magnifies the requirement for optimal complex formation to produce efficient target cell cytotoxicity. Dose titration of switches against Her2 1+ cells confirmed that the FITC LS202X/HK136X with anti-FITC CAR-T harboring CD8 hinge (EC_{50} ranging from 2.9±0.2 to 18.3±2.4 pM, Supplementary Fig. S12 and Table S5) and PNE CTBV with IgG4m-based anti-GCN4 CAR-T (EC_{50} ranging from 2.0±0.2 to 4.0±0.7 pM, Supplementary Fig S13 and Table S6) provided the greatest cytotoxicity.

To understand the basis for hinge preference in FITC and PNE-based switches, we examined the structural differences between FITC and PNE-based switches. As shown in Supplementary Fig. S14A, the LS202X and HK136X sites of FITC attachment are predicted to be approximately 24.4 Å apart, while the LCCT and HCCT grafting positions for the PNE are only 11.6 Å apart (Supplementary Fig. S15). Since the linkers used for FITC small molecule conjugation (PEG4) and PNE grafting (GGGGS) are comparable in length, the differential activity may be due to the differences in the location of FITC conjugation sites relative to the PNE grafting location. To test this possibility, we constructed a bivalent FITC switch by conjugation to residues LG212X and HK221X, which are approximately 11.6 Å apart in the constant domain, and distal to the antigen binding region. As shown in Supplementary Fig. S14B and Supplementary Fig. S16, the LG212X/HK221X FITC switch was more cytotoxic with the IgG4m hinge compared to the CD8 hinge in the FITC sCAR-T cell against Her2 1+ cells. Similarly, this new FITC switch exhibited more robust sCAR-T cell activation and greater release of inflammatory cytokines with anti-FITC sCAR-T cell harboring the IgG4m hinge (Supplementary Fig. S17). This result is similar to that of the PNE-based CTBV switch with roughly the same geometry. Collectively, these results indicate that concurrent design of the sCAR hinge and switch labeling sites is required to achieve the optimal distance and orientation for sCAR-T cell activation.

We next compared the in vitro cytotoxicity of the optimal switch/sCAR pair with that of conventional anti-Her2 CAR. The 4D5 scFv and CD8 hinge was used for the conventional anti-Her2 CAR as previously reported[26]. For this experiment 50 pM of the FITC LS202X/HK136X or PNE CTBV switch was used with the CD8 hinge FITC CAR or the IgG4m hinge CAR, respectively. As shown in Supplementary Fig. S18, sCAR-T cells killed Her2 cancer cells with comparable efficacy to the conventional CAR-Her2 across all E:T ratios tested. Both sCAR-T cells and conventional CAR-T cells showed good selectivity for Her2 cells with only minor cytotoxicity towards Her2 0 MDA MB468 cells.

To test the *in vivo* antitumor activity of each optimized sCAR-T, we first examined them in mouse xenograft models using Her2 3+ (HCC1954) and Her2 2+ (MDA MB453) breast tumors. 5×10^6 tumor cells were inoculated s.c. in the right flank of NSG mice and solid tumors grown until palpable (~300 mm^3). The half-life of Fabs in mice is approximately 1–2h[27]. However, in MDA MB435/Her2 tumor bearing mice, we observed tumor distribution of IRDye800-Fab up to 72h post i.v. injection indicating excellent tumor residence of the relatively small Fab molecule (Supplementary Fig. S19). On day 10, mice were infused i.v.

with 30×10^6 anti-FITC or anti-PNE sCAR-T cells, followed by i.v. injection of the corresponding switches every other day at 0.5 mg/kg for 14 days. Each sCAR-T cell was dosed with wild type 4D5 Fab in the control group. The conventional anti-Her2 CAR-T was included as positive control. Tumor growth was monitored for 50 days. As shown in Fig. 3A and 3B, both conventional and sCAR-T cells showed comparable tumor regression kinetics and completely eliminated both Her2 3+ and 2+ tumors by day 25; no relapse was observed during the course of the study. Treatment of sCAR-T cells with wild type 4D5 Fab had no effect on tumor growth. To test activity with lower antigen density Her2 1+ tumors, we used an orthotopic xenograft model with MDA MB231 cells. In this model, 5×10^6 tumor cells are implanted into the right fourth mammary fat pad of female NSG mice to generate tumors. Ten days after cell inoculation, we started treatment with the same dosing and schedule as the Her2 3+/2+ models described above. As shown in Fig. 3C, sCAR-T cells fully eradicated Her2 1+ tumors by day 30, and no tumor relapse occurred during the 50-days observation. The kinetics of tumor clearance were comparable to that of conventional anti-Her2 CAR-T cells. These results show that sCAR-T cells constructed with different designs can specifically target and eliminate Her2 expressing tumors with comparable efficacy to conventional CAR-T approach. Although additional studies are required to determine optimal dosing regimen, tumor distribution, persistence and other factors that affect CAR-T cell safety and efficacy, we believe these studies help facilitate application of CAR-T therapy to solid tumors for which monoclonal antibody or antibody drug conjugate therapies are not effective.

Supplementary Material

Refer to Web version on PubMed Central for supplementary material.

Acknowledgments

This work was supported by NIH grant R01 GM062159 (PGS)

Reference List

1. Barrett DM, Singh N, Porter DL, Grupp SA, June CH. Annu. Rev. Med. 2014; 65:333–347. [PubMed: 24274181]
2. Jena B, Dotti G, Cooper LJ. Blood. 2010; 116:1035–1044. [PubMed: 20439624]
3. Restifo NP, Dudley ME, Rosenberg SA. Nat. Rev. Immunol. 2012; 12:269–281. [PubMed: 22437939]
4. Grupp SA, Kalos M, Barrett D, Aplenc R, Porter DL, Rheingold SR, Teachey DT, Chew A, Hauck B, Wright JF, Milone MC, Levine BL, June CH. N. Engl. J. Med. 2013; 368:1509–1518. [PubMed: 23527958]
5. Louis CU, Savoldo B, Dotti G, Pule M, Yvon E, Myers GD, Rossig C, Russell HV, Diouf O, Liu E, Liu H, Wu MF, Gee AP, Mei Z, Rooney CM, Heslop HE, Brenner MK. Blood. 2011; 118:6050–6056. [PubMed: 21984804]
6. Rosenberg SA, Yang JC, Sherry RM, Kammula US, Hughes MS, Phan GQ, Citrin DE, Restifo NP, Robbins PF, Wunderlich JR, Morton KE, Laurencot CM, Steinberg SM, White DE, Dudley ME. Clin. Cancer Res. 2011; 17:4550–4557. [PubMed: 21498393]
7. Till BG, Jensen MC, Wang J, Qian X, Gopal AK, Maloney DG, Lindgren CG, Lin Y, Pagel JM, Budde LE, Raubitschek A, Forman SJ, Greenberg PD, Riddell SR, Press OW. Blood. 2012; 119:3940–3950. [PubMed: 22308288]

8. Maude SL, Frey N, Shaw PA, Aplenc R, Barrett DM, Bunin NJ, Chew A, Gonzalez VE, Zheng Z, Lacey SF, Mahnke YD, Melenhorst JJ, Rheingold SR, Shen A, Teachey DT, Levine BL, June CH, Porter DL, Grupp SA. N. Engl. J. Med. 2014; 371:1507–1517. [PubMed: 25317870]
9. Porter DL, Hwang WT, Frey NV, Lacey SF, Shaw PA, Loren AW, Bagg A, Marcucci KT, Shen A, Gonzalez V, Ambrose D, Grupp SA, Chew A, Zheng Z, Milone MC, Levine BL, Melenhorst JJ, June CH. Sci. Transl. Med. 2015; 7:303ra139.
10. Morgan RA, Yang JC, Kitano M, Dudley ME, Laurencot CM, Rosenberg SA. Mol. Ther. 2010; 18:843–851. [PubMed: 20179677]
11. Kakarla S, Gottschalk S. Cancer J. 2014; 20:151–155. [PubMed: 24667962]
12. Chmielewski M, Abken H. Expert. Opin. Biol. Ther. 2015; 15:1145–1154. [PubMed: 25985798]
13. Gargett T, Brown MP. Front Pharmacol. 2014; 5:235. [PubMed: 25389405]
14. Kim MS, Ma JS, Yun H, Cao Y, Kim JY, Chi V, Wang D, Woods A, Sherwood L, Caballero D, Gonzalez J, Schultz PG, Young TS, Kim CH. J. Am. Chem. Soc. 2015; 137:2832–2835. [PubMed: 25692571]
15. Ma JS, Kim JY, Kazane SA, Choi SH, Yun HY, Kim MS, Rodgers DT, Pugh HM, Singer O, Sun SB, Fonslow BR, Kochenderfer JN, Wright TM, Schultz PG, Young TS, Kim CH, Cao Y. Proc. Natl. Acad. Sci. U. S. A. 2016
16. Rodgers DT, Mazagova M, Hampton EN, Cao Y, Ramadoss NS, Hardy IR, Schulman A, Du J, Wang F, Singer O, Ma J, Nunez V, Shen J, Woods AK, Wright TM, Schultz PG, Kim CH, Young TS. Proc. Natl. Acad. Sci. U. S. A. 2016
17. Kudo K, Imai C, Lorenzini P, Kamiya T, Kono K, Davidoff AM, Chng WJ, Campana D. Cancer Res. 2014; 74:93–103. [PubMed: 24197131]
18. Tamada K, Geng D, Sakoda Y, Bansal N, Srivastava R, Li Z, Davila E. Clin. Cancer Res. 2012; 18:6436–6445. [PubMed: 23032741]
19. Urbanska K, Lanitis E, Poussin M, Lynn RC, Gavin BP, Kelderman S, Yu J, Scholler N, Powell DJ Jr. Cancer Res. 2012; 72:1844–1852. [PubMed: 22315351]
20. Dommerholt J, Schmidt S, Temming R, Hendriks LJ, Rutjes FP, van Hest JC, Lefeber DJ, Friedl P, van Delft FL. Angew. Chem. Int. Ed Engl. 2010; 49:9422–9425. [PubMed: 20857472]
21. Hudak JE, Barfield RM, de Hart GW, Grob P, Nogales E, Bertozzi CR, Rabuka D. Angew. Chem. Int. Ed Engl. 2012; 51:4161–4165. [PubMed: 22407566]
22. Cao Y, Axup JY, Ma JS, Wang RE, Choi S, Tardif V, Lim RK, Pugh HM, Lawson BR, Welzel G, Kazane SA, Sun Y, Tian F, Srinagesh S, Javahishvili T, Schultz PG, Kim CH. Angew. Chem. Int. Ed Engl. 2015; 54:7022–7027. [PubMed: 25919418]
23. Vaughan TJ, Williams AJ, Pritchard K, Osbourn JK, Pope AR, Earnshaw JC, McCafferty J, Hodits RA, Wilton J, Johnson KS. Nat. Biotechnol. 1996; 14:309–314. [PubMed: 9630891]
24. Zahnd C, Spinelli S, Luginbuhl B, Amstutz P, Cambillau C, Pluckthun A. J. Biol. Chem. 2004; 279:18870–18877. [PubMed: 14754898]
25. Milone MC, Fish JD, Carpenito C, Carroll RG, Binder GK, Teachey D, Samanta M, Lakhal M, Gloss B, Danet-Desnoyers G, Campana D, Riley JL, Grupp SA, June CH. Mol. Ther. 2009; 17:1453–1464. [PubMed: 19384291]
26. Sun M, Shi H, Liu C, Liu J, Liu X, Sun Y. Breast Cancer Res. 2014; 16:R61. [PubMed: 24919843]
27. Nguyen A, Reyes AE, Zhang M, McDonald P, Wong WL, Damico LA, Dennis MS. Protein Eng Des Sel. 2006; 19:291–297. [PubMed: 16621915]

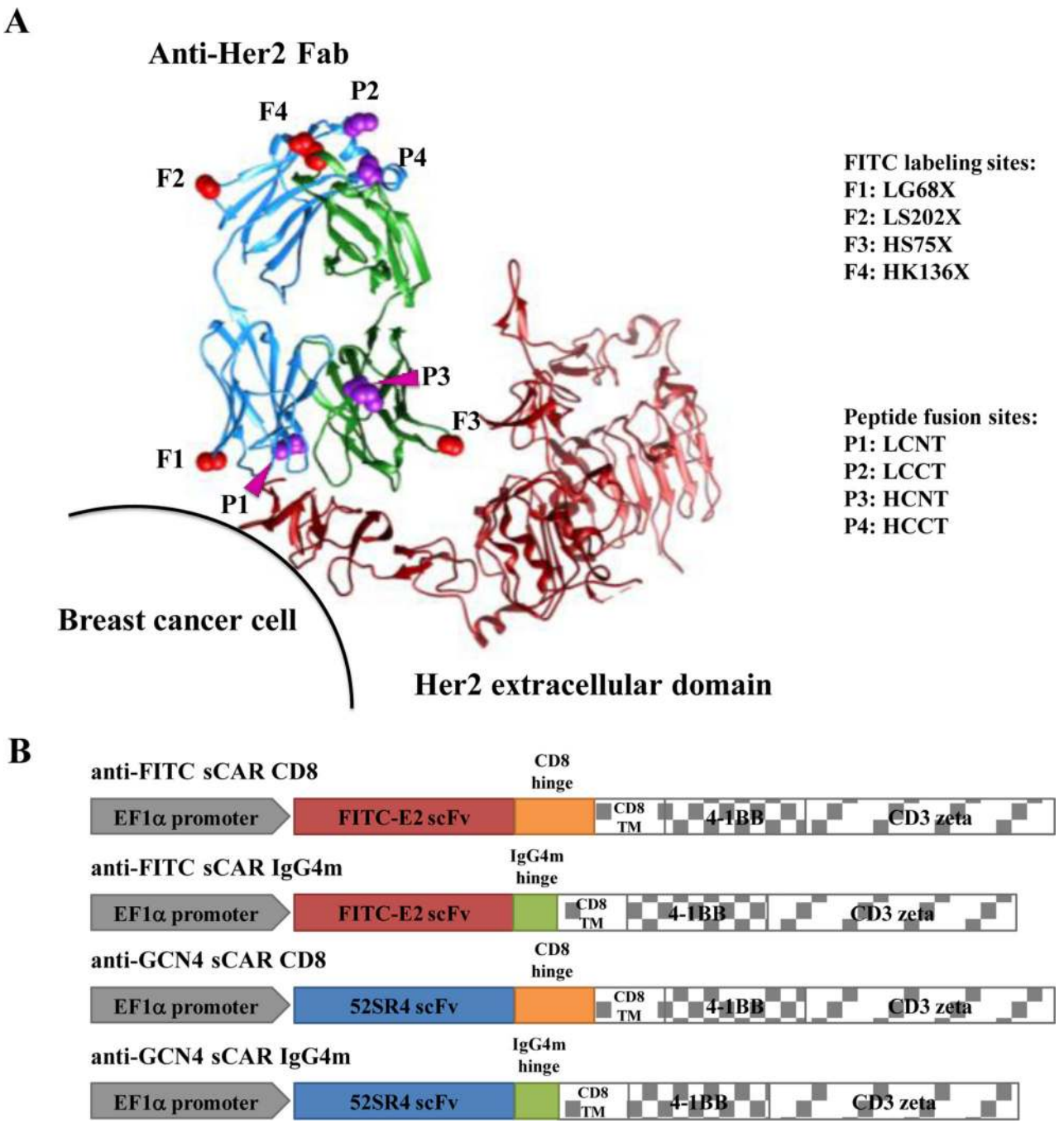

Figure 1.

Construction of FITC or PNE (GCN4) anti-Her2 Fab switches. (A) Crystal structure of the anti-Her2 Fab 4D5 bound to Her2 (red) showing the heavy (green) and light (blue) chains. Positions of the four amino acids that were individually mutated in separate constructs to encode pAzF for FITC conjugation are shown in red. The location of the two N-terminal and two C-terminal positions that were grafted with the PNE (GCN4) are shown in purple. The structure is derived from crystal structure Protein Data Bank ID 1N8Z; (B) Schematic representation of anti-FITC and anti-GCN4 sCARs containing the CD8 signaling sequence,

corresponding scFv, extracellular hinge region (CD8 or IgG4m), CD8 transmembrane domain, 4-1BB costimulatory domain and CD3ζ signaling domain.

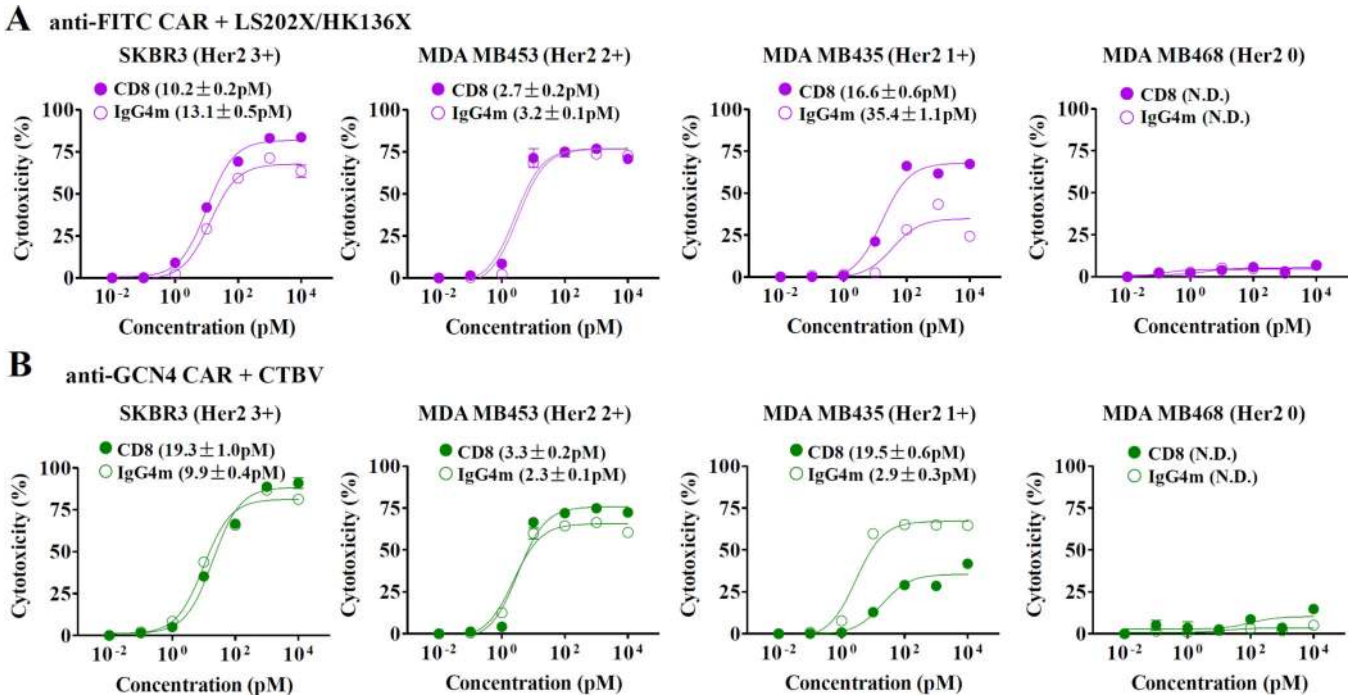

Figure 2.

In vitro cytotoxicity of sCAR-T cells harboring the CD8 or IgG4m hinges and bivalent switches. FITC (A) or GCN4 (B) specific sCAR-T cells containing different hinges were incubated with SKBR3 (Her2 3+), MDA MB453 (Her2 2+), MDA MB435 (Her2 1+) or MDA MB468 (Her2 0) cancer cells at an E: T = 10: 1 ratio with serial dilution of FITC switch LS202X/HK136X or GCN4 switch CTBV. Cytotoxicity was assayed after 24h by measuring the amount of lactate dehydrogenase (LDH) released into cultured media. The EC_{50} values (mean ± SD) were determined and listed in parenthesis in the figure legend inserts.

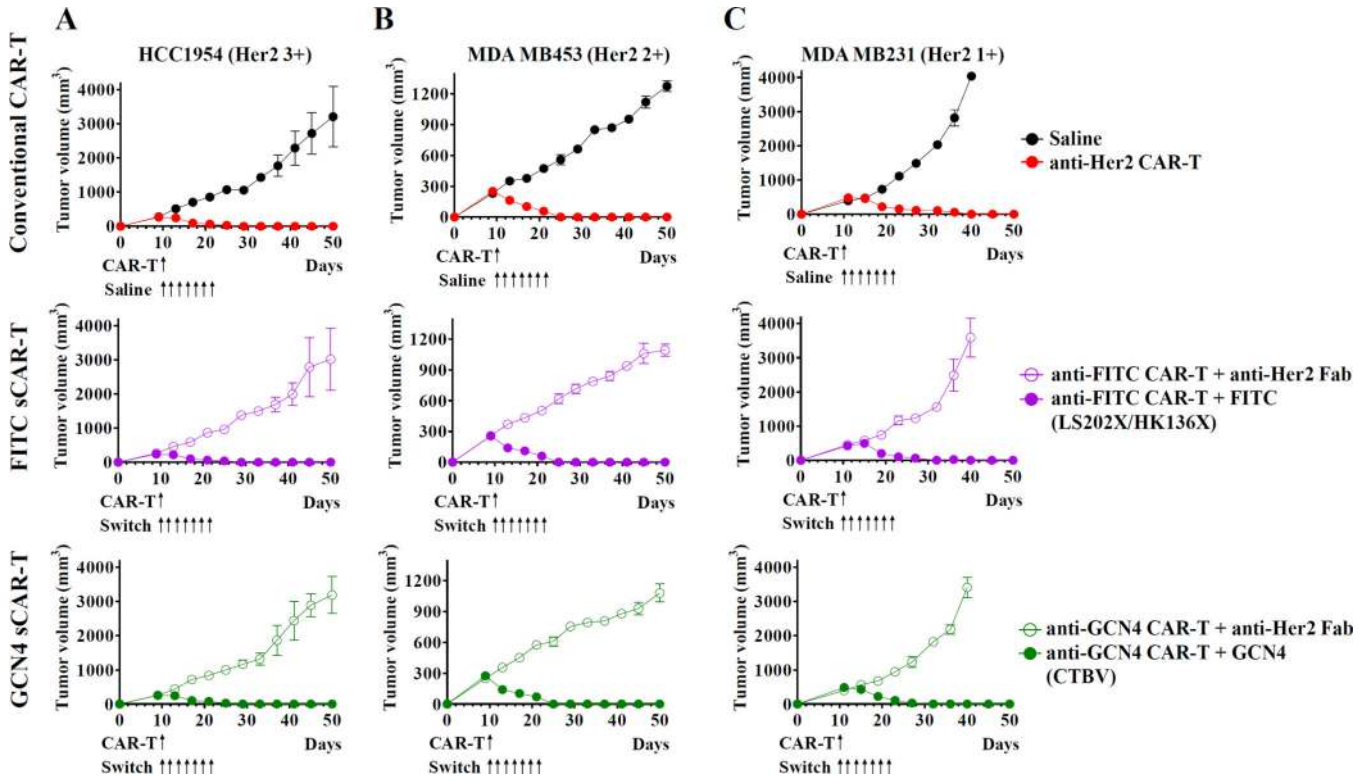

Figure 3.

In vivo antitumor efficacy of conventional anti-Her2 CAR-T and sCAR-T cell approaches in HCC1954 (A), MDA MB453 (B) and MDA MB231 (C) xenograft models. For HCC1954 or MDA MB453, 5×10^6 cancer cells were subcutaneous implanted in the right flank of female NSG mice. For MDA MB231 cancer cells, 5×10^6 cells were orthotopically implanted into the right fourth mammary fat pad of female NSG mice. Ten days later, the mice were i.v. injected with 30×10^6 CAR-T cells, followed by the dosage of switch or wild type 4D5 Fab at 0.5mg/kg every other day for 14 days. The control group received saline instead of switch and did not receive any T cells. Tumor were measured twice a week with calipers and tumor volume was calculated by W×L×H. Each data point represents tumor volume of five mice in each group. Error bars represent SD. Arrows indicate the time of CAR-T cell injection or of treatment with specific antibodies.